Sensors and Materials, Vol. 16, No. 7 (2004) 357–365
MYU Tokyo

S & M 0572

Fabrication of a Single-Walled Carbon Nanotube (SWCNT) Device Using a Novel Barricade-Confronting Electrode (BCE) Pattern for Gas Sensor Applications

Jin Woo Lee, Youngmin Choi*, Ki-Jeong Kong, Jeong-O Lee, Hyunju Chang and Beyong-Hwan Ryu

Advanced Materials Division, Korea Research Institute of Chemical Technology
P. O. Box 107, 100 Jangdong, Yuseonggu, Daejeon 305-600, Korea

(Received June 4, 2004; accepted August 30, 2004)

Key words: carbon nanotube, gas sensor, barricade-confronting electrode

A chemical gas sensor based on single-walled carbon nanotubes (SWCNTs) with improved performance has been developed using a novel barricade-confronting electrode (BCE). This arrangement comprises two adjacent electrodes with tips separated by a narrow interval (2 μm). An induced centrifugal force caused the nanotube bundles on the sample surface to shift toward the gap between electrode. The sensor device demonstrated a better detection response toward NO_2 and NH_3 gases compared with existing sensors. The sensor devices developed with a BCE show a better detection response toward NO_2 and NH_3 gases compared with nanotube sensors fabricated with an interdigitated electrode geometry. Such an enhanced sensitivity of BCE-type devices can be explained as being due to nanotube bundle-bundle contact that occurs when the electrode gap is wider than the length of nanotube bundles. A more effective dispersion of nanotubes and a narrower separation of the electrodes (< 1 μm) are expected to contribute to the realization of enhanced sensor performance.

1. Introduction

Chemical gas sensors based on single-walled carbon nanotubes (SWCNTs) have received a great deal of attention due to the excellent sensitivity of nanotubes toward various gas molecules such as NO_2,[1–3] NH_3[2,4] and others. In addition, nanotube-based

*Corresponding author, e-mail address: youngmin@krict.re.kr

sensors for carbon dioxide,[4] methane,[5] ethanol[6] and hydrogen[7,8] have also been reported. Nanotubes for sensor applications show a greater detection response and a much higher sensitivity under ambient conditions than existing metal-oxide solid-state sensors.[9,10]

For nanotube sensor applications, various electrode geometries have been developed following the development of suitable methods to disperse or align nanotubes on the sample surface. The field-effect transistor (FET) geometry uses either electrode patterning on individual SWCNTs predeposited on a substrate[1,6] (Fig. 1(a)) or in-situ nanotube growth from seed nanoparticles predeposited on neighboring electrodes[11] (Fig. 1(b)). In the former case, the processing cost is high due to the difficulties of e-beam lithography. In the latter case, the yield is very low.

Geometries formed through the nanotube mat[4,7] or drop methods,[2] on the other hand, have much higher reproducibilities. This, coupled with the ease of device fabrication, makes them highly suited sensor devices for mass production (Figs. 1(c), (d)). Interdigitated (IDE) patterns have been generally favored over other methods[2,4] (Fig. 1(d)). IDE

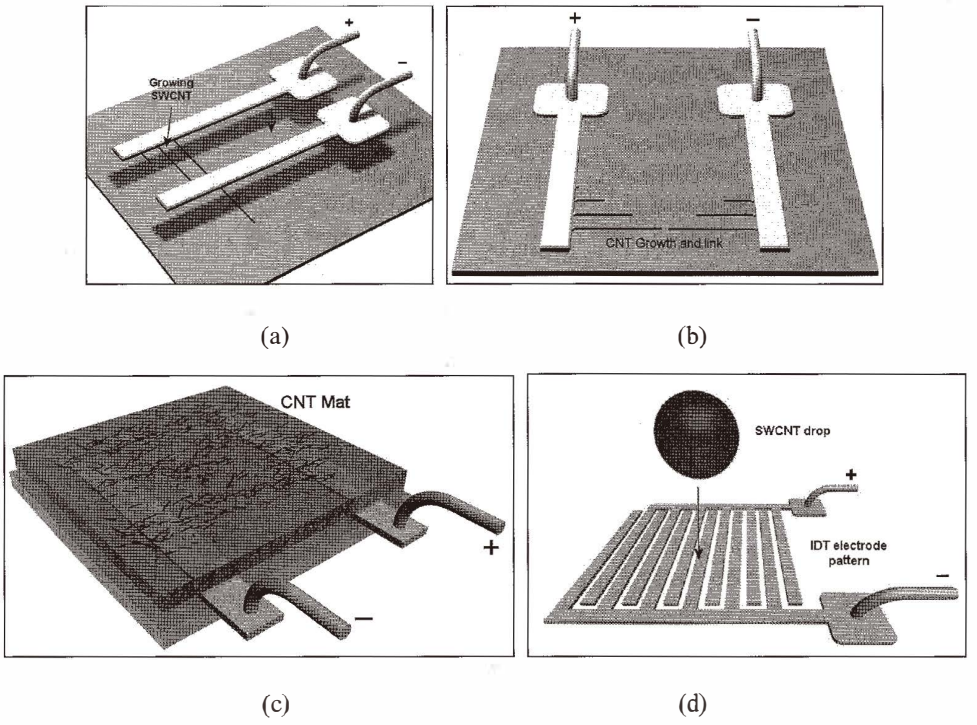

Fig. 1. Schematic illustrations reflecting typical layouts of four conventional electrode/nanotube connections. (a) Electrodes connected by predeposited seed-induced nanotubes. (b) Nanotube growth and linking from seed nanoparticles on the neighboring electrodes. (c) A mat of nanotubes deposited over coupled electrodes. (d) A nanotube suspension deposited on an interdigitated electrode (IDE) pattern.

patterns offer multiple sites for simultaneous electrical connections between electrodes and nanotubes, which may cause a reduction in the sensitivity because of the low resistance. Consequently, the performance of gas sensors fabricated from a mat or suspension of nanotubes is unable to attain the same level reached by individual nanotube-based sensors.

In an effort to overcome the low sensitivity associated with the IDE geometry, a novel electrode pad pattern, which we have termed a barricade-confronting electrode (BCE), has been developed. Moreover, the use of centrifugal force to disperse the nanotubes over the substrate surface and to attach them to the BCE-containing sensor without direct handling has been implemented for the first time. The *I-V* characteristics of the new sensor were examined in the presence of NO_2 and NH_3 gases at room temperature under computer control. The physical nature of the connection between the nanotubes and the BCE pattern was explored using high-resolution field-emission scanning electron microscopy (FE-SEM). The effectiveness of the new gas sensor fabrication method was also examined using the same technique.

2. Experimental Procedures and Results

Commercial single-walled carbon nanotubes (SWCNTs), which were manufactured through the high-pressure carbon monoxide (HiPco) process by R. Smalley at Rice University,[12] were used in gas sensors. Nanotubes dispersed in *N, N*-dimethylformamide (DMF) solution (0.025 mg/ml), a solvent long regarded as the best medium for nanotube dispersion,[13] were sonicated continuously for more than 10 h. The stability of the dispersed nanotubes over long periods of time, however, is somewhat limited.

The BCE pad pattern was fabricated through conventional photolithographic methods. A silicon oxide layer (1000 Å) was grown on a Si substrate by the thermal oxidation process, and then a pure gold electrode layer (5000 Å) was deposited over the oxide layer using the lift-off process. A schematic illustration of the electrode pattern and a scanning electron microscopy (SEM) image of an enlarged section of the confronting barricade tips, are shown in Figs. 2(a) and 2(b), respectively. The fabricated tip ends appear slightly different to the designed pattern on the mask due to the nonuniformity of the contact between the substrate and the lithography mask during UV exposure. Similary, the corresponding tip widths and interelectrode gap are also slightly different from the desired dimensions, < 2 μm and $2 \sim 3$ μm, respectively.

As illustrated in Fig. 3, a drop (1 μL) of nanotube-DMF suspension containing aproximately 0.025 μg of nanotubes was spin-coated on the fabricated electrode at high speed and the consequent centrifugal force resulted in an equal distribution of nanotubes over the sample surface. In the final step, the surface was washed with MeOH to remove any adventitious impurities (*e.g.,* amorphous carbon).

Devices with conventional IDE patterns were also fabricated for comparison with the BCE pattern deposited devices (Fig. 4(a)). In Fig. 4(b), it appears that some individual nanotubes connect two electrodes (Fig. 4(b)). However, most of the interelectrode gaps contain agglomerated nanotubes (Fig. 4(c)). The I-V curves for the IDE devices (Fig. 4(d)) exhibit typical linear characteristics of conventional IDE devices.[2] In the figure, the resistance varies from 2 Ω to 12 Ω. The multiple nanotube/electrode connections are

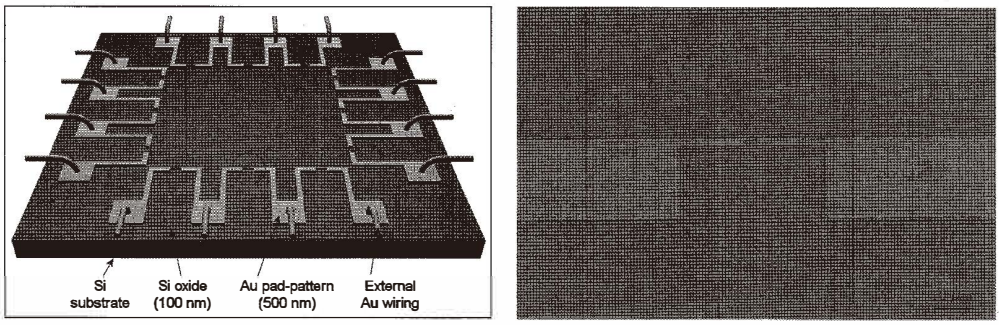

(a) (b)

Fig. 2. A schematic illustrations of a sensor device patterned with a novel barricade-confronting electrode (BCE). (a) A p-type Si wafer coated with a silicon oxide layer (100 nm) patterned with a thick (500 nm) Au electrode, in which a single wire is shared by the two nearest electrodes. (b) FE-SEM image of two adjacent electrode tips (black-circle in 2(a)).

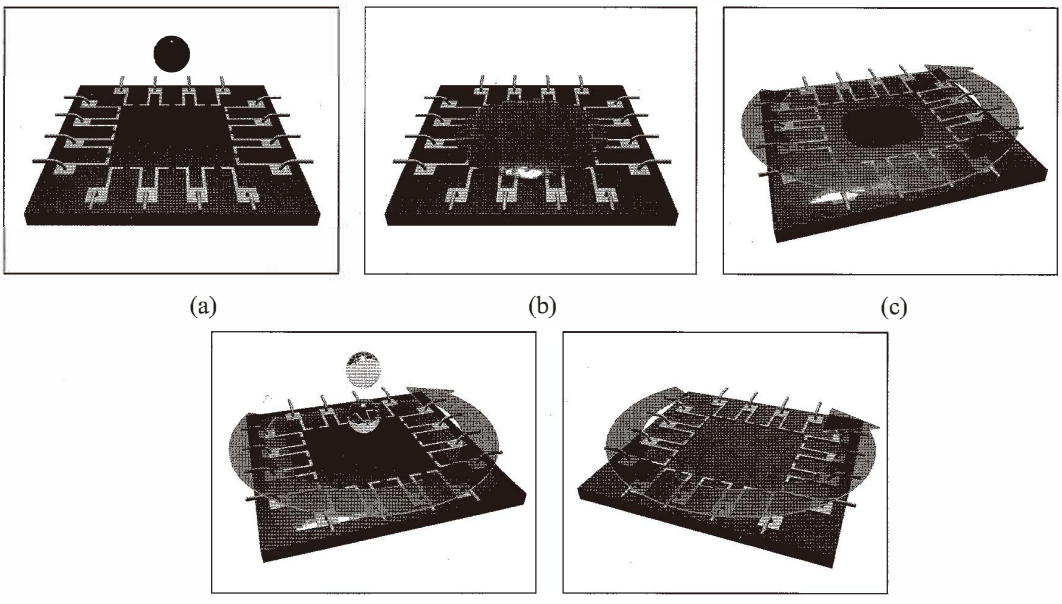

(a) (b) (c)

(d) (e)

Fig. 3. A schematic illustrations representing the procedures involved in the coating of a sensor device with a suspension of carbon nanotubes. (a) Deposition of a nanotube suspension on the sensor, (b) sample incubation for several minutes, (c) rotation-induced centrifugal force, (d) final MeOH washing step, and (e) high-speed spin drying.

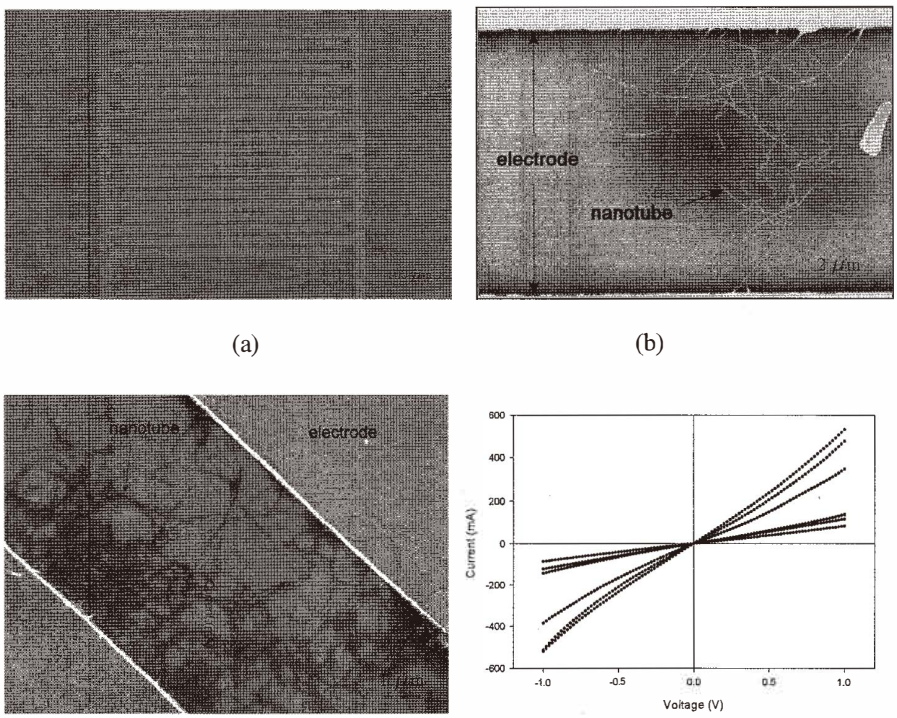

Fig. 4. (a) FE-SEM image of a conventional interdigitated electrode (IDE). The width of each electrode and the interval between two neighboring electrodes are 12 μm and 6 μm, respectively. (b) A magnified local image of 4(a) highlighting the electrical connection made by the SWCNTs located between two electrodes. (c) A gap between two electrodes occupied by agglomerated nanotubes formed as a result of poorly dispersed nanotubes in DMF solutions. (d) Typical *I*-*V* curves for IDE-patterned sensor devices with varying resistance (2 Ω to 12 Ω).

thought to be an advantage in IDE patterns, because the electrical circuit is closed in any case. However, it is very difficult to artificially control the number of connected sites via nanotubes.

Essentially, SWCNTs can be classified into two categories, metallic or semiconducting, depending on their electrical characteristics. For the fabrication of nanotube sensor devices with high performance, it is essential that the electrodes be connected via at least one semiconducting nanotube within the circuit. Several investigations[14] to isolate semiconducting nanotubes from suspensions have established that perfect separation is still quite difficult to achieve. In the case of electrode patterns with multiple sites (i.e., IDE), deposition of a mixed suspension of metallic and semiconducting nanotubes invariably produces sites connected via metallic and semiconducting nanotubes. Here, the

corresponding *I-V* curves will show metallic characteristics (Fig. 4(d)), due to the low resistance associated with these particular nanotubes.

An FE-SEM image (Fig. 5(a)) of the BCE-patterned device is shown with several SWCNTs bundles located between two neighboring electrode tips. The typical thickness of an individual nanotube is approximately 20 nm, which implies that the observed rope-like bundles cAmprise typically 20 ~ 30 nanotubes. The linking of several nanotube

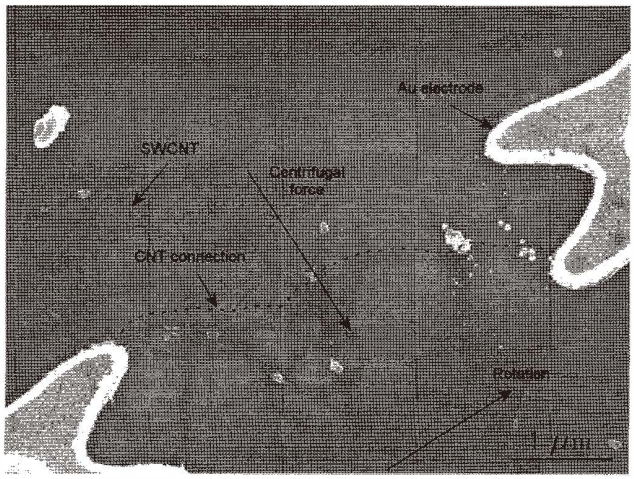

(a)

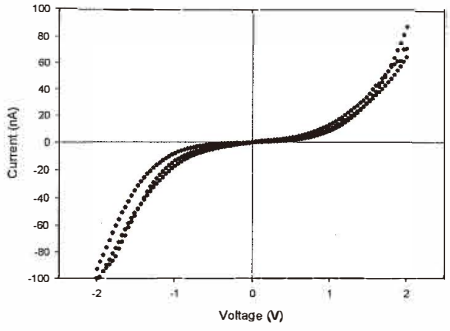

(b)

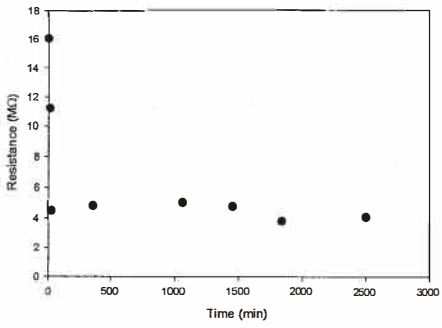

(c)

Fig. 5. (a) FE-SEM image of SWCNTs located between two electrodes of a BCE-patterned device. The arrows indicate the directions of sample rotation and the subsequently induced centrifugal force, while the dotted line indicates the aligned nanotube linkage between the electrodes. (b) Typical *I-V* curves obtained tor the BCE-patterned device. (c) Changes in resistance, measured intermittently over a period of 3000 min, demostrate the stable nature of the contacts between the nanotubes and electrodes.

bundles provides an electrical connection between the two electrodes. Here, some of the nanotubes in the links may possibly be semiconducting nanotubes, and the resulting electrical circuit may theoretically show high resistance and good sensitivity toward gas molecules. The *I-V* curves obtained for the BCE-patterned device (Fig. 5(b)) reveal significantly higher resistances (~ 20 MΩ) compared with our IDE patterned device shown in Fig. 4 and other devices.[2] To examine the reproducibility of these results, measurements were repeated under the same environmental conditions. In Fig. 5(c), the resistance is observed to fall abruptly within 1 h of the first measurement, and it eventually remains constant at around 4 MΩ. One can assume from this that the contacts between the nanotubes and electrodes become effectively stable after just 1 h. The quality of the contacts, however, is difficult to guarantee, a problem frequently encountered in the nanotube dropping method. The gas sensing experiments presented herein were all carried out under the same stable conditions at constant resistance.

The BCE-patterned device was exposed to a mixture of 100 ppm NO_2 and 1% NH_3 gas in an Ar atmosphere. As previously reported,[1,15] NO_2 gas is known to behave as a charge acceptor when its molecules are attached to nanotubes. The NH_3 molecules, on the other hand, act as charge donors. Consequently, the electrical conductance increases when the nanotubes are exposed to NO_2 gas, and decreases upon exposure to NH_3 gas. Here, we observed that exposure to NO_2 gas molecules (Fig. 6(a)) caused a 220% increase in conductance over a period of 10 min. Interestingly, the time taken to achieve 50% recovery was 100 s, while complete recovery is expected to occure over a prolonged period, in accordance with previously reported recovery times.[1,2] From the graph shown in Fig. 6(a), the changes in $\Delta G/G_o(d_{NO2})$ for the BCE-patterned device remained essentially constant during exposure to NO_2, implying good reproducibility. Indeed, the BCE-patterned device is expected to show similar recovery times if treated with other methods such as UV

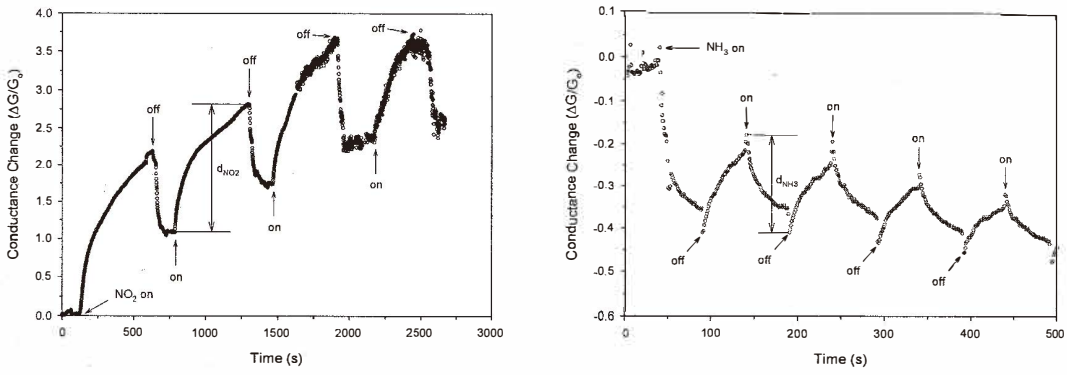

Fig. 6. Sensor responses for (a) 100 ppm NO_2 gas, and (b) 1% NH_3 gas, obtained at room temperature. Though complete reversibility is not observed, the response times are exceedingly fast.

irradiation.[2] Interestingly, exposure to NH_3 gas also caused abrupt changes in the electrical response (Fig. 6(b)). Here, the electrical conductance decreased to 36.7% of the initial value within just 50 s. While complete sensor reversibility was not observed, the reproducibility of the $\Delta G/G_o(d_{NH3})$ changes during NH_3 detection is comparable with those obtained during NO_2 sensing. Such an enhanced sensitivity of BCE-type devices toward gas molecules above IDE devices may be explained as being due to a relatively small number of nanotube bundles bridging the electrode gaps, so that the impact of metallic nanotubes is relatively smaller than for BCE-type devices. Moreover, since the electrical connections in our BCE devices are provided by chains of several nanotube bundles, we can expect that bundle-bundle contacts will also play a significant role in electrical transport in our devices. In this case, Schottky contacts resulting from bundle-bundle contacts can also explain the improved sensitivity of our devices, although detailed study of nanotube junctions is required.

In Fig. 5(a), while nanotubes seem to be attached to both Au electrodes successfully judging by the FE-SEM images, the existence of several links between nanotubes cannot be guaranteed because of the limitations of FE-SEM. The use of DMF as a solvent for producing nanotube dispersions is problematic because the resulting dispersion of nanotubes is insufficient and residues remain after the suspension is dispersed. Providing the two electrode tips are separated by a distance of or just below 1 μm, it is expected that a single nanotube bundle would be sufficient to connect the electrodes.

3. Summary

We have developed a novel barricade-confronting electrode (BCE) pad pattern for high-yield SWCNT-based gas sensing devices. The migration of nanotubes toward the interelectrode gaps was implemented by rotating the device at high speed to induce a centrifugal force, which caused the nanotubes to disperse in a controlled manner. The sensor response toward NO_2 and NH_3 gases showed good sensitivity compared with other established devices. The electrical conductance for NO_2 gas increased 220% within 10 min, while the corresponding conductance for NH_3 exhibited a 36.7% decrease. Provided better individual nanotube dispersion, and narrower interelectrode gaps (< 1 μm) are achieved, it is expected that SWCNT-based sensors with significantly improved performance will be realized.

Acknowledgements

This work was supported by MOST of Korea through the National R&D Project for Nano Science and Technology.

References

1 J. Kong, N. R. Franklin, C. Zhou, M. G. Chapline, S. Peng, K. Cho and H. Dai: Science **287** (2000) 622.

2 J. Li, Y. Lu, Q. Ye, M. Cinke, J. Han and M. Meyyappan: Nano Lett. **3** (2003) 929.

3 C. Cantalini, L. Valentini, L. Lozzi, I. Armentano, J. M. Kenny and S. Santucci: Sens. Actuators B **93** (2003) 333.
4 K. G. Ong, K. Zeng and C. A. Grimes: IEEE Sensors Journal **2** (2002) 82.
5 M. Bienfait, B. Asmussen, M. Johnson and P. Zeppenfeld: Surf. Sci. **460** (2000) 243.
6 T. Someya, J. Small, P. Kim, C. Nuckolls and J. T. Yardley: Nano Lett. **3** (2003) 877.
7 Y. M. Wong, W. P. Kang, J. L. Davidson, A. Wisitsora-at and K. L. Soh: Sens. Actuators B **93** (2003) 327.
8 O. K. Varghese, D. Gong, M. Paulose, K. G. Ong and C. A. Grimes: Sens. Actuators B **93** (2003) 338.
9 J. F. Currie, A. Essalik and J. C. Marusic: Sens. Actuators B **59** (1999) 235.
10 C. N. Xu, N. Miura, Y. Ishida, K. Matsuda and N. Yamazoe: Sens. Actuators B **65** (2000) 163.
11 Y. Wu and P. Yang: Adv. Mater. **13** (2001) 520.
12 P. Nikolaev, M. J. Bronikowski, R. K. Bradley, F. Rohmund, D. T. Colbert, K. A. Smith and R. E. Smalley: Chem. Phys. Lett. **313** (1999) 91.
13 K. D. Ausman, R. Piner, O. Lourie, R. S. Ruoff and M. J. Korobov: Phys. Chem. **104** (2000) 8911.
14 R. Krupke, F. Hennrich, H. v. Löhneysen and M. M. Kappes: Science **302** (2003) 344.
15 H. Chang, J. D. Lee, S. M. Lee and Y. H. Lee: Appl. Phys. Lett. **79** (2001) 3863.